Journal of Power Sources 385 (2018) 141–147

Contents lists available at ScienceDirect

Journal of Power Sources

journal homepage: www.elsevier.com/locate/jpowsour

Prediction of battery storage ageing and solid electrolyte interphase property estimation using an electrochemical model

T.R. Ashwin[a,*], A. Barai[a], K. Uddin[b], L. Somerville[c], A. McGordon[a], J. Marco[a]

[a] WMG, University of Warwick, Coventry, CV4 7AL, UK
[b] OVO Energy, 140-142 Kensington Church Street, London, W8 4BN, UK
[c] Jaguar Land Rover, Banbury Road, Warwick, CV35 0XJ, UK

HIGHLIGHTS

- Electrochemical model to predict storage ageing under constant temperature.
- Model uses ageing data from cells at three different SoC for validation.
- Modified correlation to account for variation in side reaction current density.
- Prediction of SEI properties such as molecular mass, density and conductivity.
- This study allows development of a combined storage-cycling framework.

ARTICLE INFO

Keywords:
Lithium-ion battery
Storage ageing
P2D model

ABSTRACT

Ageing prediction is often complicated due to the interdependency of ageing mechanisms. Research has highlighted that storage ageing is not linear with time. Capacity loss due to storing the battery at constant temperature can shed more light on parametrising the properties of the Solid Electrolyte Interphase (SEI); the identification of which, using an electrochemical model, is systematically addressed in this work. A new methodology is proposed where any one of the available storage ageing datasets can be used to find the property of the SEI layer. A sensitivity study is performed with different molecular mass and densities which are key parameters in modelling the thickness of the SEI deposit. The conductivity is adjusted to fine tune the rate of capacity fade to match experimental results. A correlation is fitted for the side reaction variation to capture the storage ageing in the 0%–100% SoC range. The methodology presented in this paper can be used to predict the unknown properties of the SEI layer which is difficult to measure experimentally. The simulation and experimental results show that the storage ageing model shows good accuracy for the cases at 50% and 90% and an acceptable agreement at 20% SoC.

1. Introduction

With increased demand for portable electronic devices, penetration of vehicles with electrified powertrains and appeal of electricity storage in grid applications, research into lithium-ion batteries (LIB) has intensified. Within the class of LIB technologies, the Nickel-Cobalt-Aluminium (NCA) cell chemistry is favoured over other chemistries such as Nickel-Manganese-Cobalt (NMC) and Nickel-Manganese-Oxide (LMO) due to longer cycle life and relatively better power delivery capabilities, which is a requirement for many modern devices. However, very few studies have suitably documented the ageing performance of this particular cell chemistry under storage, a thermodynamic equilibrium state where LIBs spend most of their time. Thus, it is important to understand the underlying nature of chemical reactions during battery storage to find the conditions that accelerate battery degradation and hence to suggest mitigation methods to enhance the life of a lithium-ion battery.

It is well established that elevated Temperature, high State of Charge (SoC), large Depth of Discharge (DoD) and large C-Rates accelerate the degradation reactions under cycling [1]. Existing ageing models such as those discussed within [2–6], are dominated by data-driven based approaches which directly relate the capacity of a battery to the stress factors or operating conditions. In the automotive industry, an electric vehicle (EV) spends 90% of the time in parked storage conditions [7,8], therefore the storage condition has a strong influence on the overall ageing of the battery. The parameters of a storage ageing

* Corresponding author.
E-mail address: A.T.Rajan@warwick.ac.uk (T.R. Ashwin).

https://doi.org/10.1016/j.jpowsour.2018.03.010
Received 19 December 2017; Received in revised form 17 February 2018; Accepted 4 March 2018

Table 1
Newman model equations.

	Governing equations	Boundary conditions
Conservation of charge		
Electrolyte phase	$\nabla.(\kappa^{eff}\nabla\phi_e) + \nabla.\kappa_D^{eff}\nabla In(c_e) + J_1 + J_s = 0$	$\left.\frac{\partial\phi_e}{\partial x}\right\|_{x=0} = \left.\frac{\partial\phi_e}{\partial x}\right\|_{x=L} = 0$
		$\left.\frac{\partial\phi_s}{\partial x}\right\|_{x=\delta^+} = \left.\frac{\partial\phi_s}{\partial x}\right\|_{x=\delta^+} = 0$
Solid Phase	$\nabla.(\sigma_{eff}\nabla\phi_s) = (J_1 + J_s)$	$-\sigma_{s,n}^{eff}\left.\frac{\partial\phi_s}{\partial x}\right\|_{x=0} = \frac{-I_{app}}{A_n}$
		$= \sigma_{s,p}^{eff}\left.\frac{\partial\phi_s}{\partial x}\right\|_{x=L} = \frac{I_{app}}{A_p}$
Conservation of lithium		
Electrolyte phase	$\frac{\partial}{\partial t}(\varepsilon_e c_e) = \nabla.(D_{e,eff}\nabla c_e) + \frac{1-t_0^+}{F}(J_s + J_1)$	$\left.\frac{\partial\phi_e}{\partial x}\right\|_{x=0} = 0,\ \left.\frac{\partial\phi_e}{\partial x}\right\|_{x=L} = 0$
Solid Phase	$\frac{\partial}{\partial t}c_s = \frac{D_s}{r^2}\frac{\partial}{\partial r}\left(r^2\frac{\partial}{\partial r}c_s\right)$	$\left.\frac{\partial c_s}{\partial r}\right\|_{r=0} = 0,\ \left.\frac{\partial c_s}{\partial r}\right\|_{r=R_s} = \frac{-J_1}{a_s F}$
Kinetics		
Electrochemical reaction rate	$J_1 = a_{n,p} i_o\left\{\exp\left(\frac{\alpha_{n,p}F\eta}{RT}\right) - \exp\left(-\frac{\alpha_{n,p}F\eta}{RT}\right)\right\}$	
Exchange current density	$i_0 = Fk_e(c_e)^{\alpha a}(c_s^{max} - c_{s,e})^{\alpha a}(c_{s,e})^{\alpha c}$	
Overpotential for the positive electrode	$\eta_p = \phi_s - \phi_e - U$	
Overpotential for the negative electrode	$\eta_n = \phi_s - \phi_e - U_n - (J_1 + J_s)\frac{G_{SEI}}{a_n}$	
Overpotential for the storage ageing reaction	$\eta_s = \phi_s - \phi_e - U_{ref} - (J_1 + J_s)\frac{G_{SEI}}{a_n}$	

electrochemical model are crucial to the development of a comprehensive ageing model for the condition seen by a battery in real world applications. The development of a storage electrochemical model is therefore an important step to understand real world ageing.

Under an electrochemical modelling framework, the ageing reactions related to static and non-static conditions reduces to a single factor-parasitic ageing side reaction intensity, therefore quantifying this side reaction is important for an electrochemical model. Unlike cycling, certain chemical reactions, like the reactions contributing to SEI formation under storage conditions, are always active and cannot be stopped. Ramadass et al. [9] presented an electrochemical-ageing model which quantifies the side reaction and exchange current density for a SONY 18650 battery under cycling. The model is very successful in predicting SEI layer growth and degradation characteristics. Hence the electrochemical model is a suitable framework with the required flexibility to facilitate a study of the chemical reactions under different storage stress factors [10].

Very few works have compared the experimentally observed degradation characteristics with the properties of the SEI layer or chemical characteristics of a battery. Specifically nobody has previously attempted to electrochemically model and experimentally validate storage ageing which, the authors believe, is a knowledge gap which needs to be filled in order to achieve a comprehensive electrochemical model for real world battery use. The modelling approach presented in this work is an attempt to correlate the parameters of the SEI layer with experimentally observed degradation characteristics which the data-driven models have failed to demonstrate so far. Therefore, theoretical or experimental SEI layer property estimations are essential for the modelling framework adopted in this work. It is important to note that a sizable amount of work has already been done to analyze SEI layer composition, for example Aurbach et al. [11], discussed different layers of various compositions, properties and conductivity.

This paper focuses on two main aspects of storage ageing predictions: SEI composition-property estimation, and introducing a new methodology to develop a single side reaction parameter to represent storage ageing. A method to parametrise an electrochemical model for any cell chemistry is presented in Ashwin et al. [12] and this is used as the basis for parametrising the electrochemical model for storage ageing at different SoCs confined to the side reaction equation proposed by Ramadass et al. [9]. A static storage experimentation is conducted where the cells are stored at constant temperature at 25 °C at three different SoC values, 20%, 50% and 90%. A sensitivity study is conducted for the first time by varying molecular weight and density of the deposit-key factors in deciding the SEI thickness. Further fine tuning of the conductivity is also needed to adjust the rate of capacity degradation. The second part of the work focuses on finding a single correlation for degradation reaction exchange current density for all storage cases considered. Often, the exchange current density for the side reaction is taken to be a constant value independent of SoC [9]. In reality, the side reaction can vary with SoC since the cell exhibits different degradation characteristics at different SoC. The correlations presented in Ramadass et al. [9] show similar degradation characteristics at lower and higher SoCs which is counter intuitive to observations. Therefore, the fitted correlation approach presented in this paper for the exchange current density for the entire SoC range can compensate for the deviation in reaction rate. The combined model is revalidated with the measured datasets to check the accuracy. This methodology can bridge the gap between data-driven and electrochemical models and the experimental data can be effectively used for parametrising an electrochemical ageing model.

To-date no one has generated a correlation based electrochemical model to predict storage ageing. To do this, the standard form of the solvent reduction side reaction was modified since it was originally derived for side reactions from cycling. In this initial work temperature is assumed constant and therefore the only variable is SoC. In this way the ageing effects can be isolated to the dependence of a single parameter which is not possible for the case of cyclic ageing. The key contribution of this work is an electrochemical model validated for storage rather than cycling which is a prerequisite for combined cycling-storage electrochemical model.

2. Governing equations

Storage is an operating condition where the externally applied current (I_{app}) and the intercalation current density (J_1) reduces to zero. This is a limiting condition for the Butler-Volmer equation which happens only when the over-potential of the intercalation reaction (η) is zero. Governing equations are presented in Table 1.

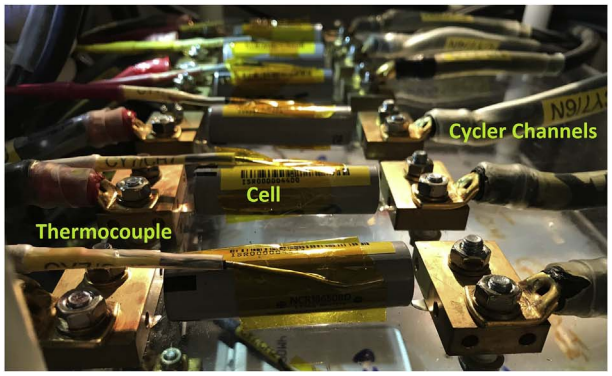

(a)

(b)

Fig. 1. Storage experimentation (a) Cells are connected with Bitrode MCV cycler for periodic characterisation (b) Cells under storage.

At the positive electrode:

$$\phi_s - \phi_e = U_p$$

where ϕ_s is the solid potential, ϕ_e is the electrolyte potential and U_p is open circuit voltage for positive electrode. The over-potential of the negative electrode is given by (ref. Table 1):

$$\eta_n = \phi_s - \phi_e - U_n - J\frac{G_{SEI}}{a_n}$$

where U_n is the open circuit voltage for negative electrode and G_{SEI} is resistance of the SEI layer. Under storage, the negative over potential η_n must be equal to zero, hence.

$$\phi_s - \phi_e - J\frac{G_{SEI}}{a_n} = U_n \tag{1}$$

This model assumes that a continuous solvent reduction reaction is happening in the negative electrode of the battery. The equation and the derivation is presented in Ramadass et al. [9]. The ageing is handled in this model with the following solvent reduction reaction kinetics:

$$J_s = -a_n i_{os} e^{(-\alpha_c f \eta_s)} \tag{2}$$

The exchange current density for the ageing reaction is represented by i_{os}. The over potential for the ageing reaction is given by (ref. Table 1):

$$\eta_s = \phi_s - \phi_e - U_{ref} - J\frac{G_{SEI}}{a_n} \tag{3}$$

Under storage, the intercalation over potential reduces to the following form:

$$\eta_s = U_n - U_{ref} \tag{4}$$

The reference voltage U_{ref}, is taken as zero in this formulation. Therefore, the side reaction current density is given by:

$$J_s = -a_n i_{os} e^{(-\alpha_c f U_n)} \tag{5}$$

The SEI layer thickness is assumed to keep increasing over time and the resistance of the SEI layer G_{SEI}, changes according to:

$$G_{SEI}\Big|_{\Delta t} = G_{SEI}\Big|_{\Delta t-1} + \frac{\delta_{SEI}}{k_{SEI}} \tag{6}$$

where δ_{SEI} is the thickness of SEI layer and κ_{SEI} is the conductivity. The battery starts with an initial resistance when t = 0. The rate of SEI layer increases over time and is proportional to the solvent reduction reaction current density and the molecular mass of the deposit M_{SEI}, and inversely proportional to the density of the deposit ρ_{SEI}.

$$\frac{\partial}{\partial t}\delta_{SEI} = -\frac{J_s M_{SEI}}{a_n \rho_{SEI} F} \tag{7}$$

The thickness keeps increasing over time according to

$$\delta_{SEI}|_{\Delta t} = \delta_{SEI}|_{\Delta t-1} + \delta_{SEI}(t) \tag{8}$$

The equations and boundary conditions are presented in Table 1. The solution algorithm for solving the system of equations is already explained in Refs. [12,13] and the procedure is not explained here for brevity.

3. Ageing experimentation & methodology

For this study, commercially available 3.03 Ah 18650 cells were used. The cells have LiC_6 negative electrode, $LiNiCoAlO_2$ positive electrode, separated by a polyethylene separator. The cells are specified to operate between 4.2 and 2.5 V. The maximum charge and discharge capability of the cells are specified as 1.5C (4.55 A) and 5C (15.15 A). However, the manufacturer recommended charging rate is at 0.3C (0.91 A) to avoid faster cell degradation. The cell has internal resistance less than 35 mΩ.

Three cells were used at each SoC, this allows for averaging the estimated capacity of the batteries and obtaining an estimate of the cell-to-cell variation (standard error). At the beginning of the test, cell capacity was measured. For the capacity measurement, cells were fully charged employing a constant current-constant voltage method using 0.3C constant current value and 4.2 V for constant voltage. Following full charge cells were rested for minimum of 2 h before discharging to 2.5 V using 0.3C, from which the cell capacity value was calculated. Following the capacity test, the SoC was adjusted to 90%, 50% and 20% SoC. In total 9 cells were used, 3 per SoC conditions. Capacity tests and SoC adjustments were performed using a Bitrode MCV cell cycler which consists of 16 battery cycling channels with 5 V maximum voltage, 100 A maximum current, 500 W total power. A Vötsch thermal chamber is used for temperature regulation of the calendar ageing conditions. All 9 cells were stored open circuit condition at 25 °C in a storage chamber as shown in Fig. 1. A capacity characterisation test was performed after 73, 139, 202 and 297 days, to calculate the remaining capacity of the cell.

4. SEI parameterisation of the model

The parametrisation of the SEI and the model development is divided into three different steps. The first step involves controlling the thickness of SEI to a desired value. The thickness of the deposit (SEI layer) can be controlled by a sensitivity study on molecular mass (M_{SEI}) and density (ρ). The second step is to control the resistance of the deposit to the experimental value so that the rate of degradation will match the measurements. The third step is to re-adjust the exchange current density for the solvent reduction reaction to accelerate or

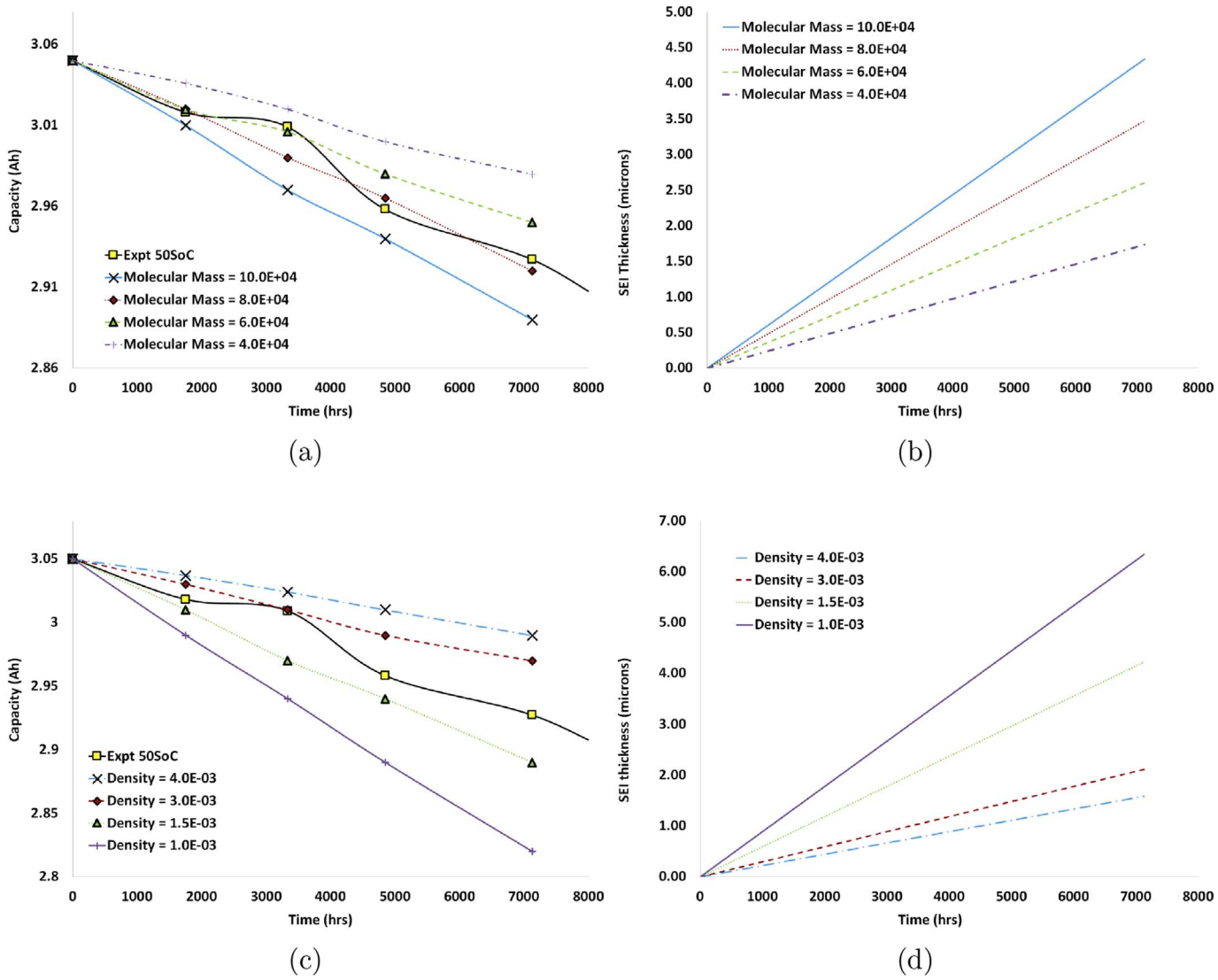

Fig. 2. Sensitivity analysis of different SEI parameters in comparison with 50% SoC measured data (a) Capacity fade with different molecular mass (kg/mol) (b) SEI thickness with different molecular mass (c) Capacity fade with different density (mol/cm^3) of the deposit (d) SEI thickness with different density of the deposit.

decelerate the capacity fade to account for the difference in SoC. The process is explained and validated as follows:

4.1. Sensitivity studies to control the thickness of SEI

A parametric study is conducted by varying the molecular mass and density which controls the rate of SEI deposited over the solid particle as shown in Equation (7). The molecular mass of the SEI deposit can change with battery chemistry, anode and cathode material and electrolyte properties or salt [14]. This model neglects any variation in SEI composition and it is collectively captured using a single molecular mass (M_{SEI}) and density (ρ).

Fig. 2a shows the variation in capacity with different molecular mass. The density of the SEI is kept constant for this simulation. A molecular mass of 10×10^4 kg/mol results in a SEI thickness of 4 microns which is not realistic. The expected maximum SEI growth is about 10–20% of the diameter of the particle therefore it is assumed that it can grow up to 3.0 microns over this time period. A preliminary attempt to measure the relative thickness of SEI can be found in Somerville et al. [15], although no actual thickness have been measured up to now. Therefore molecular masses contributing to SEI thickness above 3 microns were rejected in this model and hence a molecular mass of 7.3×10^4 kg/mol was chosen which will limit the thickness to a reasonable value of 2.5 micron over 7128 h.

A similar study presented in Fig. 2c and d showed that a higher density decreases the thickness of the deposit while a lower density increases SEI thickness. A density above 1.5×10^{-3} kg/cm^3 forms SEI below 2.5 microns over a period of 297 h of battery storage which the authors believe is a reasonable choice for this battery.

4.2. Sensitivity studies to control the resistance and rate of capacity fade

Fig. 3 shows the studies to control the rate of capacity fade with time and the 50% SoC experimental measurements. This is done by controlling the conductivity which decides the resistance induced by the SEI over the system. This study is shown in Fig. 3a and b where a lower conductivity induces a higher capacity loss and resistance increase. A conductivity of 5×10^{-8} S/cm shows much higher degradation compared to 5×10^{-6} S/cm which shows almost no degradation. The resistance of the battery is not deviating from the initial resistance of 100 Ωcm^2 whereas the 5×10^{-8} S/cm case shows a sharp increase in resistance. A general conclusion can be made that lower conductive products deposited over the particles can cause much higher resistance of the SEI layer.

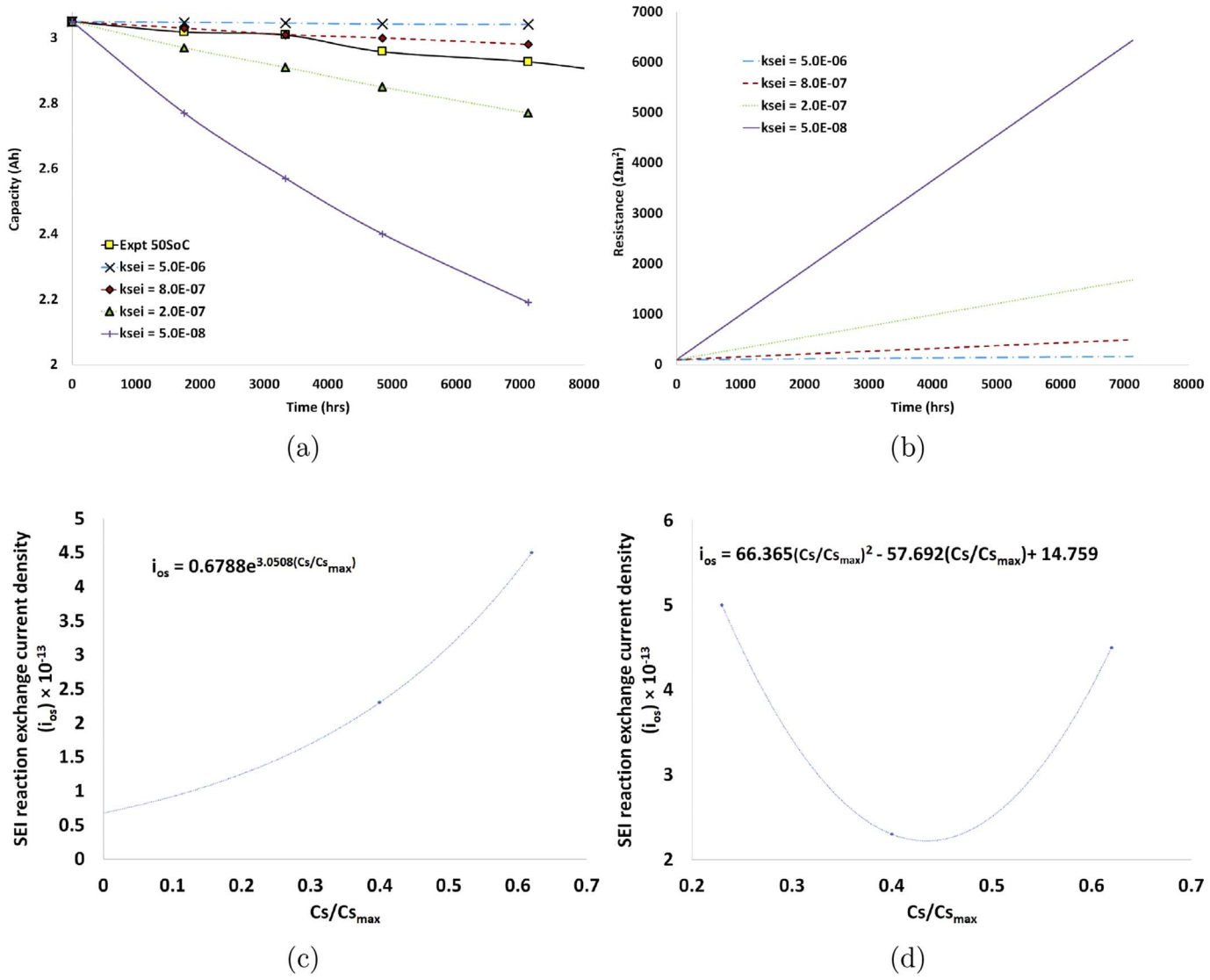

Fig. 3. Sensitivity analysis and correlation development a) Capacity fade with different conductivity of SEI b) Resistance increase of SEI with different conductivity c) Exponential fit for the side reaction exchange current density d) Parabolic fit for side reaction exchange current density.

4.3. Sensitivity studies on side reaction exchange current density

The storage exchange current density described as i_{os} in equation (2) can be treated as a measure of the chemical side reactions inside the battery. The exchange current density needs to be adjusted for the variation in the chemical reactions at different SoC, contributing to the thickening of the SEI layer.

The side reaction exchange current density given in Equation (2) reduces to the form: $-\ i_{os}\ a_n\ \ e^{-\alpha_c f U_n}$ under storage. The change in U_n at 0% SoC and 100% SoC for a graphite electrode is negligible according to the OCV data presented in Smith and Wang [16]. This relation indicates that the side reaction current density is similar at higher SoC as well as at lower SoC which is counter intuitive to the experimental observation. The general conclusion is that the degradation is weakly linked to the SoC which is a problem with the existing equation framework which needs to be rectified for accurate real world application of the model. Also this error limits the applicability of an electrochemical model for HEV drive cycle. Hence an adjustment of side reaction exchange current density is necessary to account for the higher degradation at higher SoC.

This work proposes two correlation methods for this cell chemistry based on the adjustments for exchange current density. The negative electrode stoichiometry, an indication of SoC, is selected as an independent variable. For the first trial, two SoC data sets at 50% and 90% are used for framing the correlation, therefore the 20% SoC data set can be used as a validation of the equations. Fig. 3c shows an exponential fit.

$$i_{os}\ = \left[0.6788\exp^{3.508(c_s/c_{s,max})}\right] \times 10^{-13} \tag{9}$$

A parabolic fit is also developed combining all SoC side reaction coefficients which cover the SoC range. Fig. 3d shows the parabolic fit. However this correlation includes 20% SoC data set, therefore cannot be used for validation.

$$i_{os}\ = \ [66.365(c_s/c_{s,max})^2 - 57.692(c_s/c_{s,max}) + 14.759] \times 10^{-13} \tag{10}$$

These two fits will be used to predict the capacity fade for the three storage SoC conditions.

5. Model prediction & discussion

Remaining useful capacity of the battery is predicted using the different storage models presented in Fig. 4. Each model has its own merits or demerits and the accuracy of each model varies with SoC as shown in Table 2. The results show that the independent reaction model

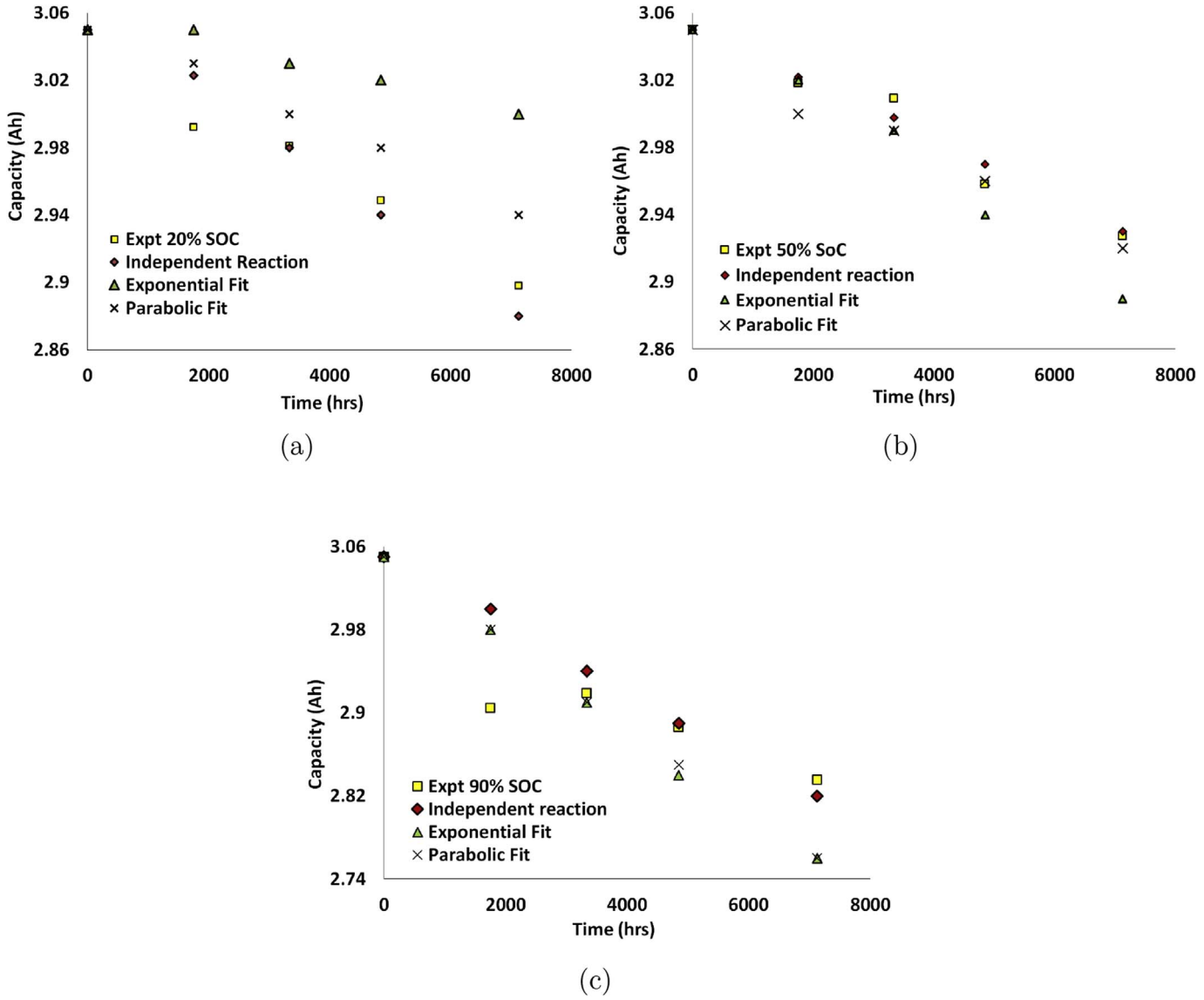

Fig. 4. Storage ageing at different SoC with independent side reaction, exponential fit and parabolic fit (a) 20% SoC (b) 50% SoC (c) 90% SoC.

Table 2
Error comparison of different models compared to experimental data for different storage SoC.

	RMSE (Ah)	RMSE (Ah)	RMSE (Ah)
	20% SoC	50% SoC	90% SoC
Independent reaction	0.018 (± 0.4%)	0.0085 (± 0.1%)	0.0495 (± 0.8%)
Exponential fit	Validation	Parametrisation	
	0.072 (± 1.8%)	0.022 (± 0.5%)	0.058 (± 1.3%)
Parabolic fit		Parametrisation	
	0.033 (0.8%)	0.013 (± 0.3%)	0.056 (± 1.2%)

is showing an overall superior accuracy compared to other two models as expected. However, all models show the highest maximum Root Mean Square error (RMSE) at 90% SoC. It had been observed that, at higher SoC, additional degradation mechanisms like lithium plating can occur leading to a decrease in the volume specific area available for intercalation and deintercalation reaction [17]. Since the model formulation only considers the SEI growth, the omission of lithium plating and other mechanisms could lead to reduced accuracy.

As explained in Section 4, the exponential fit model is formed by replacing the exchange current density (i_{os}) in equation (5) with the correlation presented in equation (9). The exponential correlation is formed with exchange current density at 50% and 90% SoC, therefore the results given by the model outside this SoC range can be considered as model prediction. In this work, model results at 20% SoC are compared with the measurement and used as a validation. The model shows an RMSE of 0.072 Ah over a prediction period of 10 months and an average deviation of ± 1.8% from experimental measurements. Researche's are trying to understand the chemical reactions when the battery is stored at different SoC. It is believed that the battery will be more susceptible to electrode corrosion and SEI dissolution which can drastically change the exchange current density at lower SoC exposing more electrode reacting area [18,19]. Therefore, to form a least error correlation, exchange current densities below 20% SoC and above 90% SoC must be chosen as a data set for forming the equation to cover the parasitic side reactions occurring at lower and higher limit of SoC. The parabolic correlation is an attempt to rectify this deficiency of the exponential model.

The parabolic model is formed with a correlation with all three SoC side reaction exchange current densities. The experimental observations at 90% SoC shows an increased capacity fade after 73 days and thereafter the reaction rate decreases. Both parabolic fit and

exponential fit models give higher errors while capturing this initial drop in reaction. The parabolic fit gives superior accuracy to the exponential fit and this is the model that is recommended.

The error comparison presented in Table 2 shows that the modified side reaction electrochemical storage ageing model is successful in predicting the degradation characteristics eliminating the influence of other parameters like temperature and DoD. The correlation for exchange current density developed in this work widens the applicability and enable the electrochemical model to be used in any operating conditions. Herein, the storage degradation characteristics of NCA chemistry cell can be captured by two types of correlation, exponential and parabolic, out of which the model with parabolic fit gives higher accuracy which is evident from the validation data presented in Table 2.

6. Conclusion

In this work, a methodology to parameterise an electrochemical model for storage ageing has been presented and validated with results from a ten month period. The existing model framework, which up to now has only been used for cycling, was found to be inadequate for storage cycling predictions. However, the addition of an adjustment of the side reaction exchange current allowed the model to accurately predict the effect of SoC on storage ageing. Two methodologies for combining SoC parameterisation points were investigated and the parabolic fit was found to give superior accuracy. The SEI properties of conductivity, molecular mass and density are difficult to measure experimentally and therefore the sensitivity study presented in this paper can be used as a guideline for any cell chemistry and be used to fine-tune the models. The modified exchange current density correlation, developed from experimental observation, can widen the applicability of an electrochemical model. Therefore, this model can in future be used for applications combining storage as well as cycling. The electrochemical model based approach combining storage and cycling offers a more physical insight into the growth and property of the SEI rather than existing data driven model approaches.

Acknowledgement

This work was funded by Innovate UK through the WMG centre High Value Manufacturing (HVM) Catapult in collaboration with Jaguar Land Rover.

Nomenclature

a	Active surface area per electrode unit volume ($3\varepsilon/\Lambda$) (cm^{-1})
A	Electrode plate area (cm^2)
c	Volume-averaged concentration (mol cm^{-3})
D	Diffusion coefficient ($cm^2\ s^{-1}$)
G	SEI resistance ($\Omega\ cm^2$)
i_o	Exchange current density for intercalation reaction (A cm^{-2})
i_{os}	Exchange current density for solvent reduction reaction (A cm^{-2})
I_{app}	Applied current (A)
J_1	Reaction current for intercalation reaction (A cm^{-3})
J_s	Reaction current for solvent reduction reaction (A cm^{-3})
L	Cell width (cm)
M	Molecular weight (kg mol^{-1})
r	Radial coordinate (cm)
t	Time (s)
t^0	Transference number
U	Open Circuit Voltage, OCV (V)
V	Cell voltage (V)

Greek symbols

A	Charge-transfer coefficient
δ	Thickness (cm)
ε	Volume fraction of domain
Λ	Particle radius (cm)
P	Density (kg cm^{-3})
K	Conductivity of electrolyte (S cm^{-1})
κ_D	Diffusivity (A cm^{-1})
σ	Solid phase conductivity (S cm^{-1})
ϕ	Volume averaged potential (V)

Superscript & subscript

e	Electrolyte phase
eff	Effective
max	Maximum
n, p	Negative and Positive electrode
ref	Reference
s	Solid phase
sur	Surface quantity
−	To the left of an interface
+	To the right of an interface

Abbreviations

SEI	Solid Electrolyte Interphase
SoC	State of Charge
DoD	Depth of Discharge

References

[1] K. Uddin, R. Gough, J. Radcliffe, J. Marco, P. Jennings, Appl. Energy 206 (2017) 12–21.
[2] M. Broussely, S. Herreyre, P. Biensan, P. Kasztejna, K. Nechev, R. Staniewicz, J. Power Sources 97 (2001) 13–21.
[3] E. Sarasketa-Zabala, I. Gandiaga, L. Rodriguez-Martinez, I. Villarreal, J. Power Sources 272 (2014) 45–57.
[4] M.B. Pinson, M.Z. Bazant, J. Electrochem. Soc. 160 (2013) A243–A250.
[5] I. Baghdadi, O. Briat, J.-Y. Delétage, P. Gyan, J.-M. Vinassa, J. Power Sources 325 (2016) 273–285.
[6] A. Eddahech, O. Briat, J.-M. Vinassa, Energy 84 (2015) 542–550.
[7] M. Burgess, N. King, M. Harris, E. Lewis, Transport. Res. F Traffic Psychol. Behav. 17 (2013) 33–44.
[8] M. Burgess, M. Harris, C. Walsh, S. Carroll, S. Mansbridge, N. King (2013).
[9] P. Ramadass, B. Haran, P.M. Gomadam, R. White, B.N. Popov, J. Electrochem. Soc. 151 (2004) A196–A203.
[10] M. Doyle, T.F. Fuller, J. Newman, J. Electrochem. Soc. 140 (1993) 1526–1533.
[11] D. Aurbach, B. Markovsky, I. Weissman, E. Levi, Y. Ein-Eli, Electrochim. Acta 45 (1999) 67–86.
[12] T.R. Ashwin, A. McGordon, W.D. Widanage, P.A. Jennings, J. Power Sources 341 (2017) 387–395.
[13] T.R. Ashwin, G. Narasimham, S. Jacob, Int. J. Heat Mass Tran. 54 (2011) 3357–3368.
[14] S. Malmgren, K. Ciosek, M. Hahlin, T. Gustafsson, M. Gorgoi, H. Rensmo, K. Edström, Electrochim. Acta 97 (2013) 23–32.
[15] L. Somerville, J. Bareño, P. Jennings, A. McGordon, C. Lyness, I. Bloom, Electrochim. Acta 206 (2016) 70–76.
[16] K. Smith, C.-Y. Wang, J. Power Sources 160 (2006) 662–673.
[17] J. Vetter, P. Novák, M. Wagner, C. Veit, K.-C. Möller, J. Besenhard, M. Winter, M. Wohlfahrt-Mehrens, C. Vogler, A. Hammouche, J. Power Sources 147 (2005) 269–281.
[18] M. Saulnier, A. Auclair, G. Liang, S. Schougaard, Solid State Ionics 294 (2016) 1–5.
[19] L. Boulet-Roblin, M. El Kazzi, P. Novák, C. Villevieille, J. Electrochem. Soc. 162 (2015) A1297–A1300.